



Research Paper

Assessing the microbial communities using metagenomics approach from the ink gland of marine nudibranch *Kalinga ornata*

Accepted 26th May 2023

ABSTRACT

Marine nudibranchs biomes are diverse and considered to be precursor for many products if it was rightly approached. These changes may also have consequences on pigments and biomolecules production considering that molluscan ink is a key component. In this study, we describe the taxonomic diversity and metabolic functions of bacterial and fungal communities present in *Kalinga ornata* ink gland as an initiative. To accomplish this goal, we collected ink glands from *K. ornata* and employed a shotgun metagenomic approach to sequence the microbial DNA. Our metagenomic analyses revealed that the habitats shared both beneficial and opportunistic microbial species. Regarding the metabolic diversity, we found that genes pertaining to the metabolism of amino acids, fatty acids, and nucleotides as well as genes involved in secondary metabolism were enriched in forest soils. On the other hand, genes related to miscellaneous functions were next to the most abundant. These results suggest that the metabolic function of microbes found in this organism differs, though differences are not related to taxonomy. Finally, we propose that the implementation of environmentally friendly practices by the pharmaceutical and other industries may help to maintain the microbial diversity and ecosystem functions associated with natural habitats.

Ramachandiran Sivaramakrishnan*,
Selvaraj Uthra, Thirukumar Sangeshwari
and Muthuvel Arumugam

Faculty of Marine Sciences, Centre for Advai
Studies in Marine Biology, Annamalai Unive
Parangipettai – 608502, Tamil Nadu, India.

*Corresponding author. E-mail:
siva.krish08@gmail.com

Key words: Marine nudibranch, metagenomics, microbiomes, ink gland.

INTRODUCTION

An understanding of microbial and/or their genes interaction in various environmental niches represents a major challenge for the environmental microbiologist. However, in marine environments, more than 99% of the microorganisms cannot be cultured with readily available technologies. The development of culture independent techniques which bypass the need for isolation and laboratory cultivation of individual species has fundamentally changed the direction of study. This regulation has its roots in the analysis of 16S rRNA genes composed from the environment (Olsen *et al.*, 1986). Instead of sorting only rRNAs, these techniques are now competent of handling genomic DNA isolated from naturally occurring microbial communities and the study referred to as metagenomics (Handelsman *et al.*, 1998). The associated endosymbionts of marine sponges are found

to be a wealthy source of marine natural products (Cragg, 2009). A topical example was the study by the Wagner group, which employed 16S rRNA tag pyro sequencing method to examine the bacterial mixture associated with three sponge of different species and the surrounding seawater. More than 250,000 sequences were generated, which were later on aligned to twenty-three bacterial phyla, representing a much higher diversity than earlier reported study (Webster, 2009). Metagenomic analyses have also been accounted from corals (Cooney, 2002; Frias-Lopez, 2004; Wegley, 2007) with classified fungal sequences accounting for 38% and the remaining recognized sequences aligning to bacteria (7%), phage (3%), eukaryotic viruses (2%), and archaea (1%). The known bacterial sequences were most parallel to the class of *Actinobacteria*, *Proteobacteria*, *Firmicutes*, *Cyanobacteria*.

This marine mollusc represents a variety of bioactive molecules from associated microbes. Thus, the present study was carried out to prospect the microbiomes of *Kalinga ornata* for which the metagenomics approach was employed to study the presence of microbial communities in the ink gland.

METHODOLOGY

Min-ION: PCR amplification and bar-coding

DNA preparation and the library, the Oxford Nanopore protocol 1D PCR bar-coding amplicons (SQK-LSK108) followed the method of Delgado et al. (2019). Specifically, approximately 1500bp fragments was amplified for full 16s rRNA gene & 400bp ITS region. DNA was amplified using a nested PCR with a first round to add the 16s rRNA / ITS gene primer sets and a second round to add the barcodes. In this study, we used 16s rRNA / ITS region universal primer and amplified 16s rRNA / ITS gene. This universal set of primers commonly used when assessing Bacterial /Fungi diversity. The primers used in this study are listed below:

27F - 5' AGAGTTTGATCMTGGCTCAG 3'

1492R - 5' TACGGYTACCTTGTTACGACTT 3'

ITS1 - 5' TCCGTAGGTGAACCTGCGG 3'

ITS4 - 5' TCCTCCGCTTATTGATATGC 3'

The 16s rRNA / ITS gene primers with the Oxford Nanopore Universal Tag were added to their 5' end. The universal tag was 5'-TTTCTGTTGGTGCTGATATTGC-3' for forward primers and 5' ACTTGCTGTGCTCTATCTTC-3' for reverse primers. These universal tags enable the second barcoding PCR using the PCR Barcoding kit (EXP-PBC096). In the first round, 25 µL of PCR mixture contained initial DNA sample (5 µl or as per the concentration), 12.5ul Long amp Taq 2X Master Mix (New England Biolabs), 1ul forward primer and 1ul reverse primer and makeup to 25 µl final volume nuclease free water added. The PCR thermal profile consisted of an initial denaturation step for 30s at 94°C, followed by 30 cycles for 15s at 94°C, 15s at 55°C annealing temperature, 90s at 72°C for extension, and a final step for 10 min at 72°C. To assess possible reagent contamination, each PCR reaction included a no template control (NTC) sample, which did not amplify.

In the second round, PCR mixture (25 µl) contained 0.5 nM of the first-round PCR product, 12.5ul Long amp Taq 2X Master Mix (New England Biolabs) and 2 µl of each specific barcode (EXP-PBC001) as recommended in the Oxford Nanopore protocol 1D PCR bar-coding amplicons (SQK-

LSK108). The PCR thermal profile consisted of an initial denaturation step for 30s at 94°C, followed by 15 cycles for 15s at 94°C, 15s at 62°C for annealing, 90s at 72°C for extension, and a final extension step for 10 min at 72°C. Following each PCR round, a clean-up step using AMPure XP beads at 0.5X concentration was performed to discard short fragments as recommended by the manufacturer. DNA quantity was assessed using Qubit fluorimeter. A final equimolar pool containing 1ug of the bar-coded DNA samples in 45 uL of DNase and RNase free water were used to prepare the sequencing library.

MinION: Library preparation and sequencing

The Ligation Sequencing Kit 1D (SQK-LSK108) was used to prepare the amplicon library loaded into the MinION, following the instructions of the 1D PCR barcoding amplicon protocol of ONT. Input DNA sample was 1 µg of the barcoded DNA pool in a volume of 45 and 5 µL of DNA CS (DNA from lambda phage, used as a positive control). The DNA was processed for end repair and tailing using the NEB Next End Repair / dA-tailing Module (New England Biolabs). A purification step using Agencourt AMPure XP beads (Beckman Coulter) was performed and approximately the expected 700 ng of total DNA were recovered as assessed by Qubit quantification. For the adapter ligation step, 0.2 pmol of the end-prepped DNA (approximately 200 ng of our 1,500 bp fragment) were added in a mix containing 50 µL of Blunt/TA ligase master mix (New England Biolabs) and 20 µL of adapter mix; they were incubated at room temperature for 10 min. Further, purification step was performed using Agencourt AMPure XP beads (Beckman Coulter) and Adapter Bead Binding buffer provided on SQK-LSK108 kit to finally obtain the DNA library. We prepared the pre-sequencing mix (12 µL of DNA library) loaded by mixing with Library Loading beads (25.5 µL) and running buffer with fuel mix (37.5 µL). We used Spot ON Flow Cell Mk I (R9.4) (FLO-MIN106). After the quality control, we primed the flow cell with a mixture of Running Buffer with fuel mix (RBF from SQK-LSK108) and Nuclease-free water (500 µL + 500 µL). Immediately after priming, the nanopore sequencing library was loaded in a drop wise fashion using the spot-on port. As soon as the library was loaded, we initiated a standard 48h sequencing protocol using the MinKNOW software.

MinION: Data pre-processing and bioinformatics analysis

Base calling was performed using the Guppy v2.3.1 and demultiplexing and adapters trimming using Pore chop v0.2.4 software.

EPI2ME analysis workflow allows users to perform genus-level identification from single reads; with access to

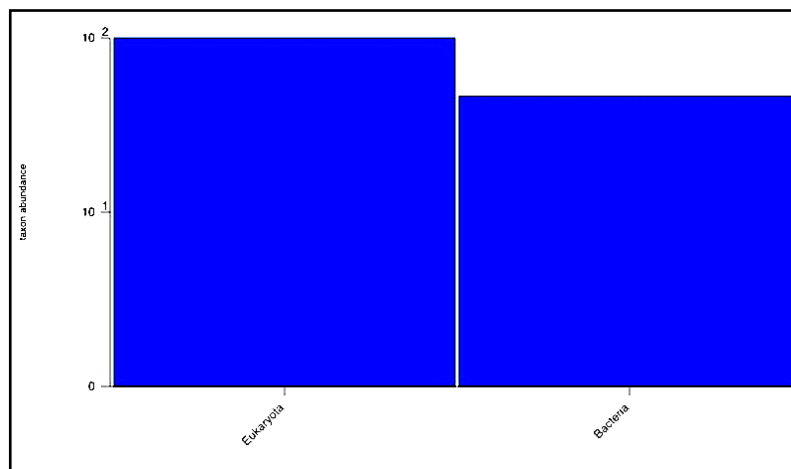


Figure 1: Taxonomical hit distribution - domain wise.

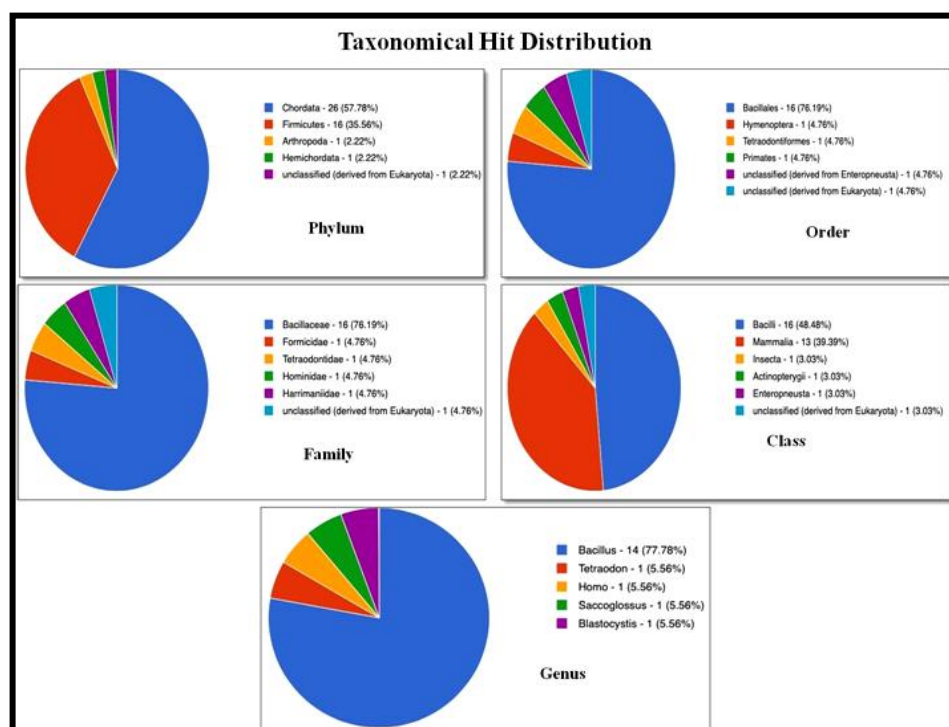


Figure 2: Taxonomical hit distribution of phylum, order, family, class, and genus.

base called files for detailed investigations at the species and sub-species level. The phylogeny analysis of query sequence with the closely related sequence of blast results was performed followed by multiple sequence alignment tool. The workflow was designed to BLAST base sequence against the NCBI database, which contains sequences from different organisms. Each read is classified based on % coverage and identity.

This step aids in identifying the pathogens in a mixed sample or understanding the composition of a microbial community.

RESULTS

Metagenomics analysis of ink gland

Taxonomical hit distribution domain-wise of microbes from ink gland showed that eukaryota (63.83%) followed by bacteria (36.17%) dominated the ink gland of *K. ornata* (Figure 1). Among eukaryota, chordata (57.78%) was considered as maximum. The taxonomic hit distribution revealed the abundance in the order; class, family, and genus as represented in (Figure. 2). In addition, the 9 most

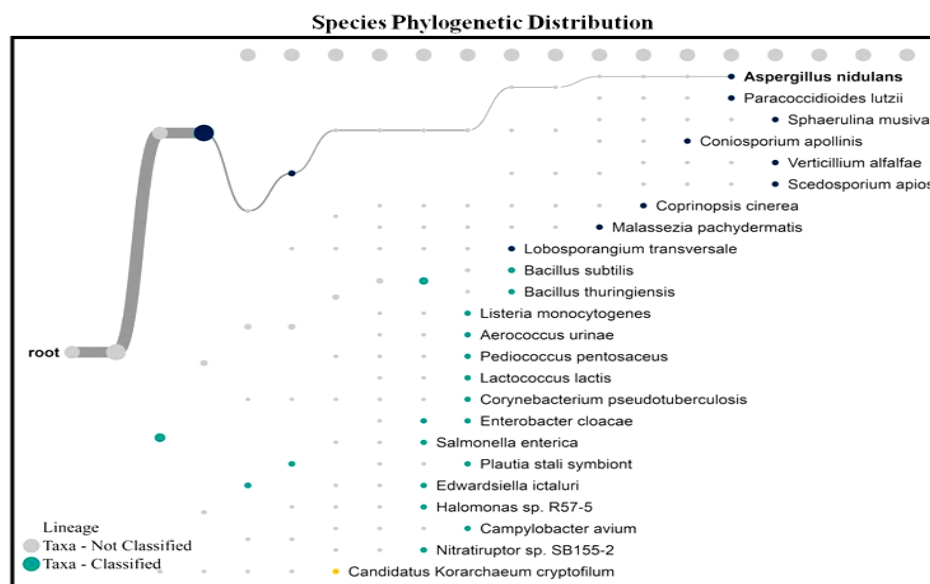


Figure 3: Taxonomical hit distribution of species.

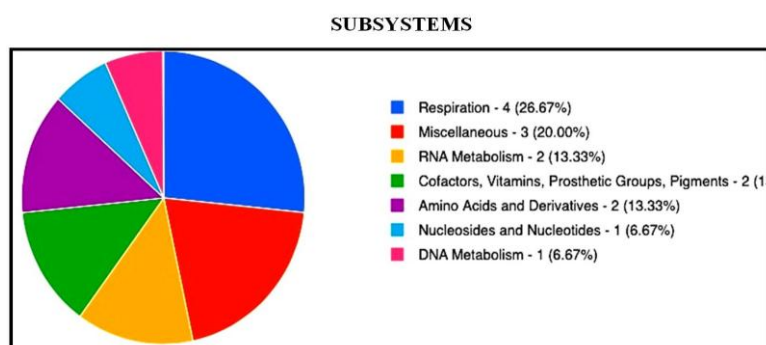


Figure 4: Functional hit categories – subsystems.

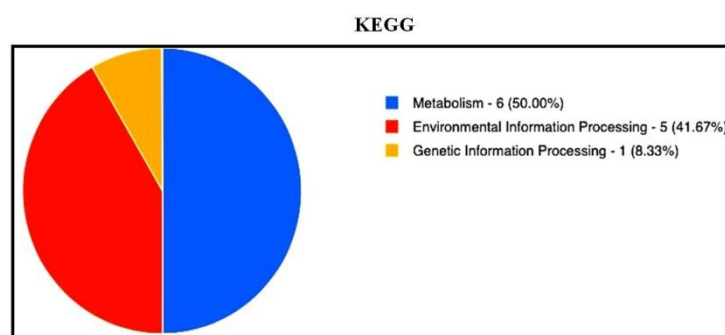


Figure 5: Functional hit categories – KEGG.

prominent species were found to be *Aspergillus nidulans*, *Paracoccidioides lutzii*, *Sphaerulina musiva*, *Coniosporium apollinis*, *Verticillium alfalfa*, *Scedosporium apios*, *Coprinopsis cinerea*, *Malassezia pachydermatis*, and *Lobosporangium transversale*, represented in Figure 3.

Functional metabolic categories related to microorganisms found in the ink gland were presented and the most common functional categories were included in

sequences related to respiration, 26.67% (that is, clustering based on subsystems) as shown in Figure 4. KEGG functional analysis revealed that proteins encoding metabolism accounted for 50%, followed by environmental information processing at 41.67% and genetic information processing at 8.33%, as shown in (Figure 5). Whereas in COG analysis, the proportion of poorly characterized proteins was 62.07%, and known metabolic proteins

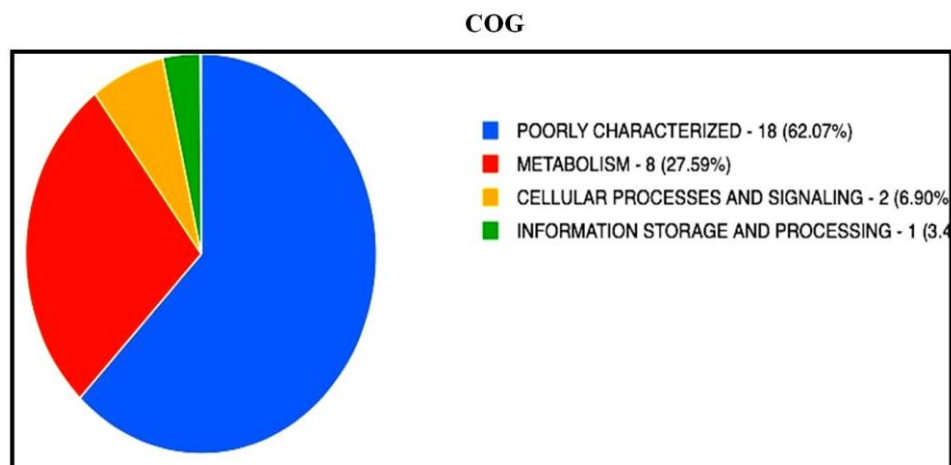


Figure 6: Functional hit categories – COG.

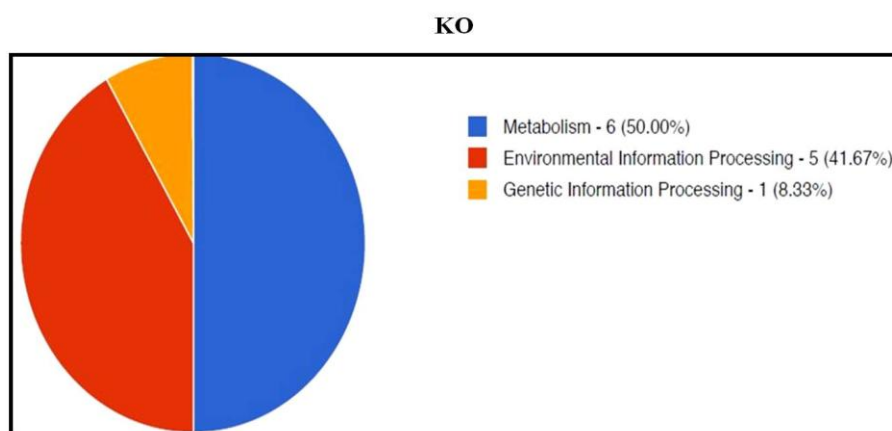


Figure 7: Functional hit categories – KO.

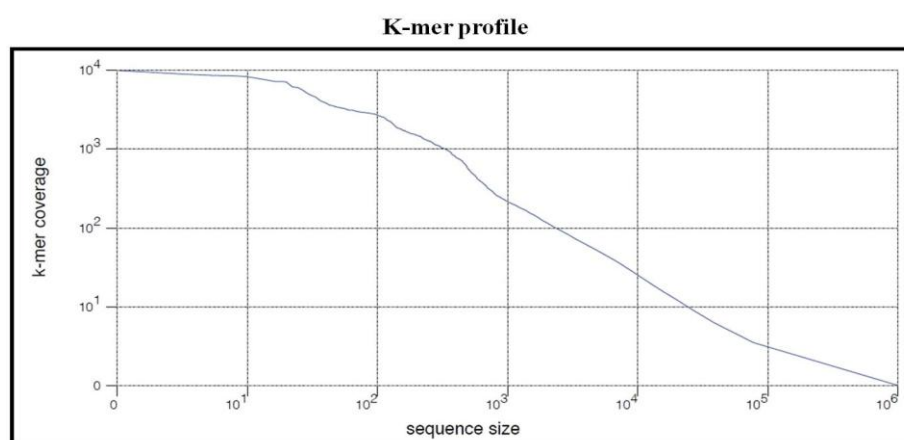


Figure 8: K-mer profile of ink gland metagenomes.

27.59% (Figure 6). KO analysis was found to mimic that of KEGG functional analysis (Figure 7).

K-mer rank abundance graph plots the k-mer coverage as a function of abundance rank with the most abundant

sequences at the left (Figure 8). The rare fraction curve of Figure 9 shows the annotated species richness. This curve was plotted using the total number of distinct species annotations as a function of the number of sequences

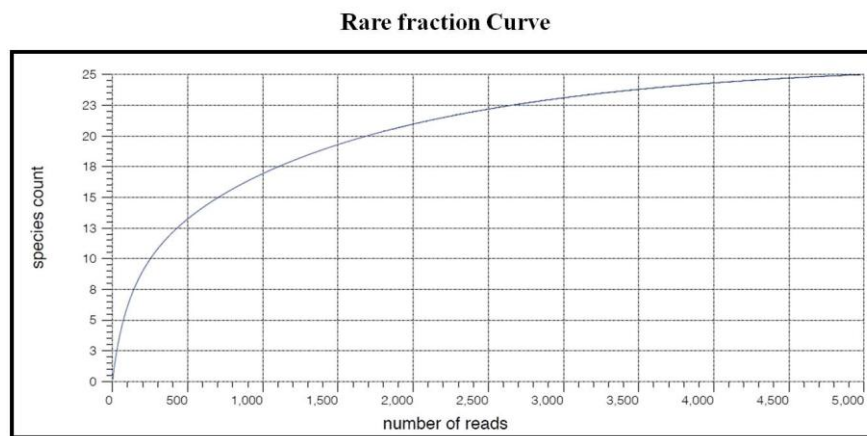


Figure 9: Rare fraction curve for the ink gland metagenomes.

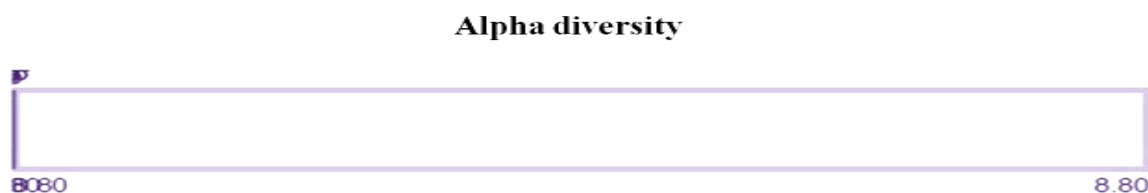


Figure 10: α -diversity of ink gland metagenomes.

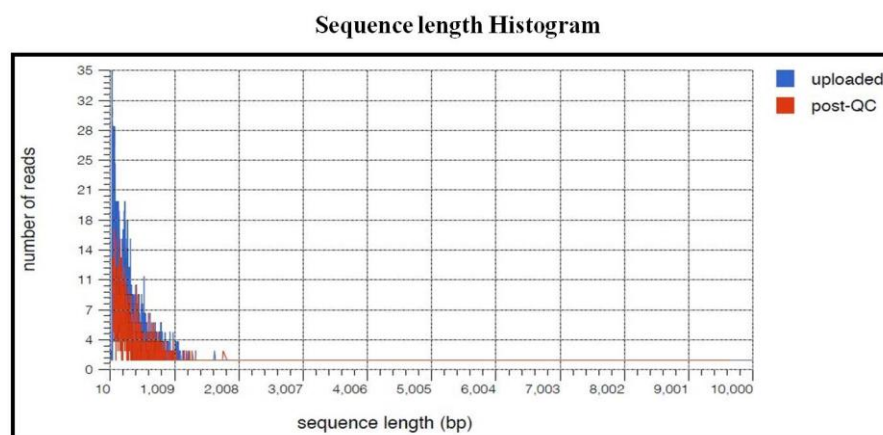


Figure 11: Sequence length histogram of ink gland metagenomes.

sampled. On the left a steep slope indicated that a large fraction of species diversity remains yet to be discovered. Sampling curves generally rose very quickly at first and then leveled off toward an asymptote as fewer new species are found per unit of individuals collected. These rarefaction curves were calculated from the table of species abundance. The curves represented the average number of different species annotations for subsamples of the complete data set.

The image showed the range of α -diversity values in the present study. The min, max, and mean values are shown with standard deviation ranges σ and 2σ in different shades. The α -diversity of this metagenome was shown in

red (Figure 10). α -diversity summarizes the diversity of the organisms with a sample number. The α -diversity of annotated samples could be estimated from the distribution of the species-level annotations. The α -diversity of this data set was found to be 9 species. However, we could not find any significant differences in alpha-diversity between habitats.

Additionally, sequence length histogram showed the distribution of sequence lengths in base pairs for this metagenome. Each position represented the number of sequences within a length bp range. The data used in these graphs was based on raw upload and post QC sequences (Figure 11). Lastly, sequence GC distribution (Figure 12)

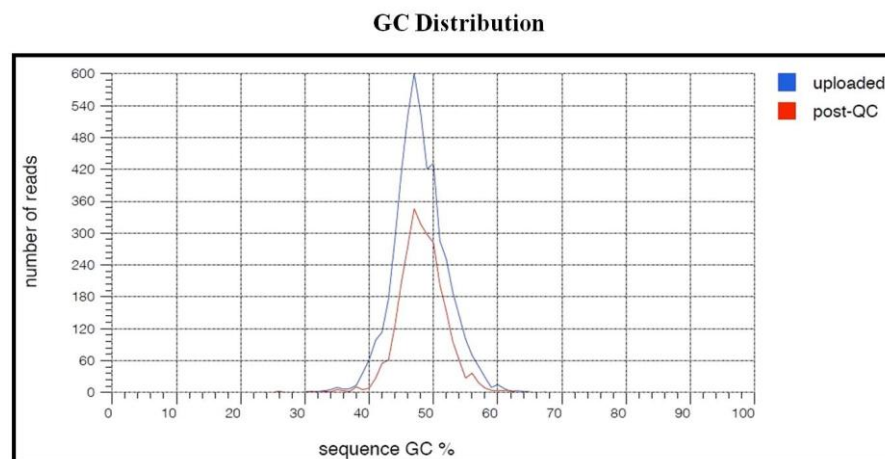


Figure 12: GC distributional hits of ink gland metagenome.

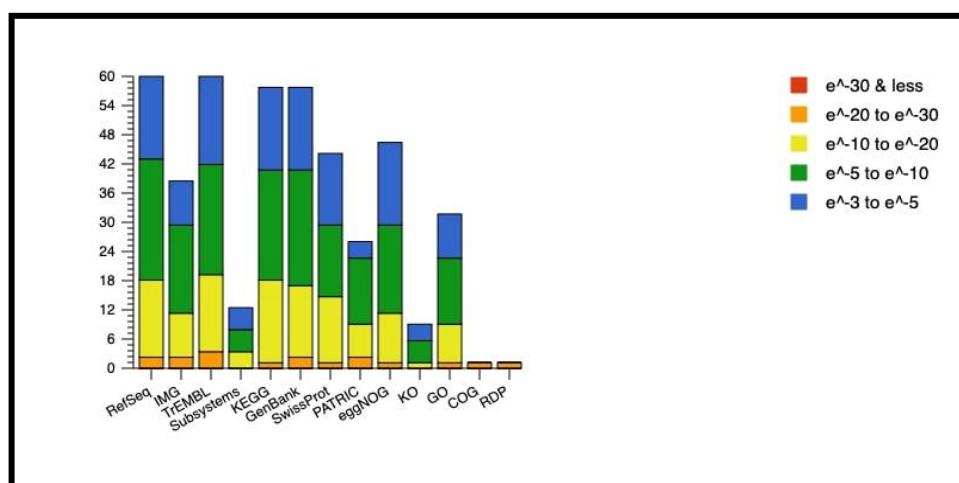


Figure 13: Source hit distribution of ink gland metagenomes.

showed the GC percentage for the current metagenome study. Each position represented the number of sequences within a GC percentage range. The data used in these graphs was based on raw upload and post QC sequences.

Additionally, source hit distribution of Figure 13 displays the number of hits in the different databases listed. These include protein databases with functional hierarchy information and ribosomal RNA databases. The bars representing annotated reads are closed by e-value range. Different databases depicted different numbers of hits and also different types of annotation data (Figure 13).

DISCUSSION

To assess the microbial community present in the ink gland of *K. ornate*, metagenomic approach based on the construction of 16S rDNA libraries was used. For assessing the quality of the data set, the nucleotide position histogram is a good starting point. The uploaded base pair

(bp) count was 1,581,841; sequence count was 4,745; mean sequence length as 333±351 bp; mean GC percent was 48±4% respectively; whereas, post QC base pair count was 944,172bp; sequences count 2,568; mean sequence length 368±384bp; mean GC percent as 49±4%; predicted protein features 2,674; predicted rRNA features 1,136; identified protein features 55; identified rRNA features 1, respectively. In addition, predicted features from ink gland revealed that genes which encode for unknown protein, annotated protein and ribosomal RNA were of 1901 (74.03%), 127 (4.95%) and 540 (21.03%).

Taking the taxonomic classes into account, bacilli types (48.48%) are common, followed by mammals (39.33%). In terms of order, bacilli species account for 76.19% of the abundance, followed by Hymenoptera and other orders. In terms of family, the Bacillaceae are the largest group with 76.19%, followed by Formicidae, Tetraodontidae, Hominidae and Harrimonidae. Finally, bacillus accounted for 77.78% of the genus classification, followed by tetraodan (5.56%), homo (5.56%), saccoglossus (5.56%),

and blastocystis (5.56%). The sequences related to respiration accounted for 26.67% of all functional categories (that is, clustering based on subsystems), followed by miscellaneous (20.00%), metabolism of amino acids and derivatives (13.33%), other RNA metabolism (13.33%), co-factors (vitamins and prosthetic groups), pigments (13.33%), nucleosides and nucleotides (6.67%), and DNA metabolism (6.67%). Similarly, in a study conducted by Noor Ahmad et al. (2018) from the microbial communities associated with wild *Labroids dimidiatus*, using the 16S rDNA-based metagenomics analysis 1,426,740 amplicon sequence reads corresponding to 508 total OTUs were obtained from three metagenomics libraries. A total of 36 different classes and 132 families were identified as well. The major five phyla from the above said research were *Proteobacteria*, *Bacteroides*, *Firmicutes*, *Actinobacteria*, and *Fusobacteria*.

However, in our study only firmcutes was observed as the second highest phyla from the ink gland of *K. ornata*. Nudibranch, a marine mollusk, is constantly exposed to aquatic environment, hence the largely synchronized bacteria composition on the skin was common. Beyond the bios of the surrounding waters, distribution of microbial communities in the stomach and other internal organs may also be largely influenced by the type of diet fed by the animal (Dabarca et al., 2013). Also, *Lactobacillus* sp., *Lactococcus* sp., *Enterococcus* sp., *Shwenella* sp., *Bacillus* sp., *Aeromonas* sp., *Vibrio*, *Enterobacter* sp., *Pseudomonas* sp., *Clostridium* sp. and *Kocuria* sp. were identified in the above-mentioned research. Similarly, in our study, the species distribution of ink gland (*Aspergillus nidulans*, *Paracoccidioides lutzii*, *Sphaerulina musiva*, *Coniosporium apollinis*, *Verticillium alfalfa*, *Scedosporium apios*, *Coprinopsis cinerea*, *Malassezia pachydermatis*, *Lobosporangium transversal*, and *Bacillus subtilis*) were considered to be classified taxa whereas, *Bacillus thuringiensis*, *Listeria monocytogenes*, *Aerococcus urinae*, *Pediococcus pentosaceus*, *Lactococcus lactis*, *Corynebacterium pseudotuberculosis*, *Enterobacter cloacae*, *Salmonella enteric*, *Plautia stali* symbiont, *Edwardsiella ictaluri*, *Halomonas* sp R57-5, *Campylobacter avium*, *Nitratiruptor* sp SB155-2, *Camdidatus korarchaeum cryptofolium* were considered not classified taxa.

Cardinale et al. (2006), had earlier reported that the differences in the structure of bacterial societies of the surroundings and the host organisms might simply be opportunistic infection, rather than symbiotic relationship. In another study, metagomics analysis conducted on marine coastal invertebrates revealed that a total of 1,854,290 raw reads were generated, 4,36,154 were trimmed and considered to be high-quality reads with a range of 25,637 to 38,463 reads per sample (Kim et al., 2017). In the present study, *A. nidulans* was found to be abundant as compared with other microbes obtained. *A. nidulans* plays an important role in cellulose production through protein kinase A. Thus, the aforementioned study has demonstrated that protein kinase A is involved in the

synthesis of hydrolytic enzyme in *A. nidulans*. It appears that this protein kinase blocks the glucose pathway hence increasing hydrolytic enzyme secretion and inducing the usage of cellular storages (Assis et al., 2015). *B. subtilis* found in the present study has many applications towards medical sciences and human life as well (Tannock, 2001). The basic applications include probiotics, generation of bacterial vaccine either as antigen bearers or as antigen cellular manufactories, growth promoter in diets related to broilers (Sen et al., 2012; Deshpande et al., 2011; Ferreira et al., 2005). In another study, *B. subtilis* E20, a probiotic bacterium, was demonstrated to have the potency to increase growth in white shrimp by enhancing the action of the digestive enzymes and food attraction (Liu et al., 2009). *Coniosporium apollinis* is a rock inhabiting fungus isolated from the marble in the sanctuary of delos (Sterflinger et al., 1997). Hence, this ink gland comprises both symbiotic and opportunistic microbes.

ACKNOWLEDGEMENTS

The authors are grateful to the Ministry of Earth Sciences (MoES), [G4 (2)/14748/2016] under 'Drugs from the sea' program for their financial support. We also express gratitude to DST under the program 'National Facility for Marine Natural Products and Drug Discovery', CAS in Marine Biology, Annamalai University for providing necessary support during this study.

REFERENCES

- Olsen GJ, Lane DJ, Giovannoni SJ, Pace NR, Stahl DA (1986). Microbial ecology and evolution: a ribosomal RNA approach. *Annu Rev Microbiol.* 40: 337-365.
- Handelsman J, Rondon MR, Brady SF, Clardy J, Godman RM (1998). Molecular biological access to the chemistry of unknown soil microbes: a new frontier for natural products 5: 245-249.
- Cragg GM, Grothaus PG, Newman DJ (2009). Impact of natural products on developing new anti-cancer agents. *Chemical Reviews.* 109, 3012-3043.
- Webster NS, Taylor MW, Behnam F, Luckner S, Rattei T, Whalan S, Horn M, Wagner M (2009). Deep sequencing reveals exceptional diversity and modes of transmission for bacterial sponge symbionts. *Environ. Microbiol.*
- Cooney RP, Pantos O, Le Tissier MD, Barer MR, O'Donnell AG, Bythell JC (2002). Characterization of the bacterial consortium associated with black band disease in coral using molecular microbiological techniques. *Environ. Microbiol.* 4, 401-413.
- Frias-Lopez J, Klaus JS, Bonheyo GT, Fouke BW (2004). Bacterial community associated with black band disease in corals. *Appl. Environ. Microbiol.* 70, 5955-5962.
- Wegley Lm, Edwards R, Rodriguez-Brito B, Liu H, Rohwer F (2007). Metagenomic analysis of the microbial community associated with the coral *Porites astreoides*. *Environ. Microbiol.* 9, 2707-2719.
- Delgado B, Serrano M, González C, Bach A, González-Recio O (2019). Long reads from Nanopore sequencing as a tool for animal microbiome studies.
- Nurul A, Muhammad DD, Okomoda VT, Nur A (2019). 16S rRNA-Based metagenomic analysis of microbial communities associated with wild *Labroids dimidiatus* from Karah Island, Terengganu, Malaysia. *Biotechnology reports (Amsterdam, Netherlands)*, 21, e00303.
- Dabarca L, Sieiro AC, Álvarez M (2013). Change in food ingestion induces

- rapid shifts in the diversity of microbiota associated with cutaneous mucus of Atlantic salmon *Salmo salar*. *J. Fish Biology*. 82(3):893-906.
- Cardinale BJ, Srivastava DS, Duffy JE, Wright JP, Downing AL, Sankaran M, Jouseau C (2006). Effects of biodiversity on the functioning of tropic groups and ecosystems. *Nature* 443, 989-992.
- Hyewon Kim, Hyunkyong Kim, Hee Seung Hwang, Won Kim (2017). Metagenomic analysis of the marine coastal invertebrates of South Korea as assessed by Illumina MiSeq, *Animal Cells and Systems*, 21:1, 37-44.
- Assis De LJ, Ries LNA, Savoldi M, Reis dos TF, Brown NA, Goldman GH (2015). Leandro Jose de Assis Laure Nicolas Annick Ries Marcela Savoldi Thaila Fernanda dos Reis Neil Andrew Brown Gustavo Henrique Goldman *Aspergillus nidulans* protein kinase A plays an important role in cellulase production. *Biotechnol Biofuels*. 8: 213.
- Tannock GW (2001). Molecular assessment of intestinal microflora. *Am J Clin Nut*. 73: 410-45.
- Sen S, Ingale SL, Kim YW, Kim JS, Kim KH, Lohakare JD (2012). Effect of supplementation of *Bacillus subtilis* LS 1-2 to broiler diets on growth performance nutrient retention caecal microbiology and small intestinal morphology. *Res Vet Sci*. 93: 264-8.
- Deshpande G, Rao S, Patole S (2011). Progress in the field of probiotics. *Curr Opin Gastroenterol*. 27: 13-18.
- Ferreira LC, Ferreira RC, Schumann W (2005). *Bacillus subtilis* as a tool for vaccine development: From antigen factories to delivery vectors. *An Acad Bras Cienc*. 77: 113-24.
- Liu CH, Chiu CS, P-L Ho, Wang SW (2009). Improvement in the growth performance of white shrimp, *Litopenaeus vannamei*, by a protease-producing probiotic, *Bacillus subtilis* E20, from natto. *Journal of Applied Microbiology*, 107:
- Sterflinger KR, Baere De, GS. Hoog De, Wachter R. De, Krumbein WE, Haase G (1997). *Coniosporium perforans* and *C. apollinis* two new rock inhabiting fungi isolated from marble in the sanctuary of delos. *Antonie van Leuvenhoek* 72: 349-363.

Cite this article as:

Sivaramakrishnan R, Uthra S, Sangeshwari T, Arumugam M (2023). Assessing the microbial communities using metagenomics approach from the ink gland of marine nudibranch *Kalinga ornata*. *Acad. J. Microbiol. Res*. 11(1): 012-020.

Submit your manuscript at

<http://www.academiapublishing.org/ajmr>